**THE TIMELINE OF EARLY LUNAR BOMBARDMENT CONSTRAINED BY THE EVOLVING COMPOSITIONS OF DIFFERENTLY-AGED MELT.** T. Liu[1], G. Michael[2] and K. Wünnemann[1,2], [1]Museum für Naturkunde Berlin, Leibniz Institute for Evolution and Biodiversity Science, Germany (tiantian.liu@mfn.berlin), [2]Freie Universität Berlin, Germany.

**Introduction:** The early bombardment history of the Moon provides fundamental constraints on the final stages of planetary accretion, the period that is usually referred to as Late Accretion from 4.5 to 3.8 billion years ago. The impactor flux (i.e., impact rate function) during this stage was much more intense than it is at the present day, but the overall timeline, i.e., how the impactor flux rate evolved with time is still a matter of debate [1-3].

The overall timeline of the early bombardment is commonly modelled with three types of shapes of the decay of the impactor flux as a function of time: tail-end [4-6], sawtooth [7] and terminal cataclysm (or late heavy bombardment) [8, 9]. Since the occurrence time of impact events is recorded in their generated melt, the heated materials caused by the high temperature of the cratering process, the distribution of differently-aged melt provides an essential tool to constrain the impactor flux rate [10-12]. By using a spatially resolved impact mixing model [12], we estimate the composition of the differently-aged melt after long-term impact mixing under the different timelines of the bombardment during late accretion. By comparing the model-derived melt content with the actual data, we provide constraints on the impactor flux rate of the early bombardment history.

**Methods:** We use the Monte Carlo method to simulate the cumulative impact mixing considering three scenarios of the decay of the impact rate (terminal cataclysm, tail-end, and sawtooth). We choose the Neukum flux model [4] to represent the tail-end scenario. The impact rate of the terminal cataclysm scenario is calculated by adding a prominent Gaussian peak at 3.9 Ga to the tail-end impact rate [11]. The impact rate of the sawtooth scenario is directly adopted from [12]. With the knowledge of lunar chronology and production functions [4], the sequence of impact events is generated for three different types of impact rate function. Impact events of different sizes randomly occurred over the Moon in chronological sequence. For each impact, the processes of melting (re-melting), excavation and ejecta deposition are simulated. Each impact heats a certain amount of material producing new melt with the age of its occurrence time.

The occurrence of basin-forming events in our model is not random but follows the inventory and stratigraphic age of known basins [13]. The timing is calculated according to the *N*(20) crater densities measured by [13] using the chronology function according to the three different bombardment rates. To distinguish from the radioisotopic ages, the calculated basin ages are referred to as "**crater-derived age**".

**Results:** The modeling results are compared with the radioisotopic datings of lunar samples.

*Global distribution.* The various impact rate functions result in different frequencies of small impacts and distinct crater-derived ages of basins for the given *N*(20) values. Figure 1b presents the distribution of differently-aged melt in the near-surface considering various shapes of the bombardment timeline. The most remarkable difference is the distribution of general peaks. While both the tail-end and the sawtooth present three peaks at 3.9, 4.1 and 4.3 Ga, the terminal cataclysm results in only one prominent peak at around 3.8 Ga. Another significant difference is the probability relative to the most abundant melt (i.e., the prime peak). Compared to the tail-end scenario, the probability of 4.1 and 4.3 Ga melt is significantly smaller than the prime peak of 3.9 Ga in the sawtooth scenario.

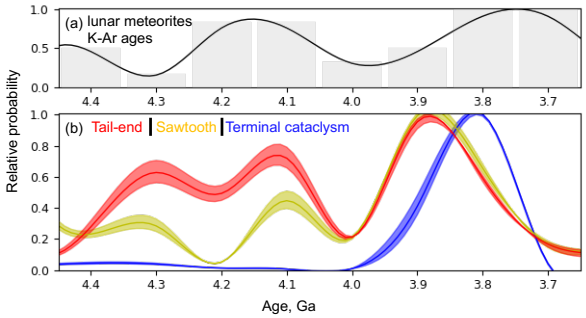


Figure 1. Globally average distribution of differently-aged melt in the near surface. (a) K-Ar datings of lunar meteorites [11]. (b) the model-derived melt compositions (top 5 meters)

Because K–Ar system is highly sensitive to shock metamorphism and heating caused by the meteoritic bombardment, K-Ar datings have been frequently performed while analyzing impact-related components. Michael et al. (2018) [11] summarized 94 K-Ar datings of clasts of the lunar highland rocks in lunar meteorites. The histogram (Figure 1a) shows that the K–Ar age distribution of the considered meteoritic highland rocks has no prominent peak around 3.9 Ga as it is typical for the Apollo highland rocks. Instead, we see a broad and low concentration between 3.7 and 4.4 Ga with three gentle peaks at 3.75, 4.15 and 4.4 Ga.

Comparing the model-derived melt composition with the isotopic datings of lunar meteorites suggests that tail-end and sawtooth scenarios match better than the terminal cataclysm scenario regarding the number and magnitude of general peaks.

*Distribution at Apollo sampling sites.* The melt composition is spatially varied and shows regional particularities [12]. The melt composition at sampling sites may, thus, allow for further constraining the impact rate of the early bombardment. Figure 2 shows the integrated melt composition of the Apollo sampling sites. Being different from the estimates of the global average, the feature of a single-sharp-peak not only occurs in the terminal cataclysm scenario but also in the sawtooth view. Instead, the melt composition under the tail-end impact rate displays a distinctly different pattern, especially for ages >4.1 Ga: In addition to the primary peak at 3.9 Ga, the magnitude of two secondary peaks at 4.25 and 4.35 Ga is significant as well. The distinct features of the estimated distribution of old melt imply that we can use the actual data of old melt composition in returned samples to further distinguish between the sawtooth and the tail-end scenario.

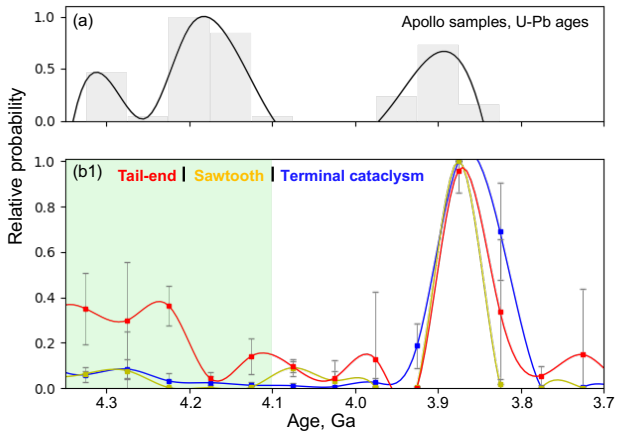


Figure 2 Integrated melt composition at Apollo sampling sites. (a) U-Pb datings of Apollo samples [16]. (b) The model-derived melt compositions (top 5 meters).

U-Pb datings appear to better conserve information on the early bombardment history [14, 15]. To assess the current U-Pb age data on zircons of Apollo samples, Vanderliek et al. (2021) [16] compiled >1000 zircon spot analyses from the literature and considered grains of unambiguously impact-related origin. Their results (Figure 2a) show that zircons at most landing sites have been affected by impact events between 3.9 and 4.3 Ga, and samples show three impact-related zircon age populations at 3.9, 4.15 and 4.3 Ga.

Compared with the model-derived melt composition, as in the globally averaged estimates (Figure 1), the U-Pb data are also difficult to reconcile with the hypothesis of the terminal cataclysm. More importantly, given the distinct patterns of model-derived melt composition between the tail-end and the sawtooth scenario (Figure 2), the distribution of the U-Pb data favors the tail-end scenario over the sawtooth.

**Discussions and conclusions:** To constrain the timeline of the early bombardment history, we investigate the outcome of melt composition under three types of impact rate scenarios (tail-end, sawtooth, and terminal cataclysm) using our spatially-resolved impact mixing model. Our results suggest that the timeline of the early bombardment history more likely to have the tail-end shape rather than the sawtooth or terminal cataclysm decay, with the terminal cataclysm being the least likely.

A robust test of the late cataclysm hypothesis requires an accurate absolute age for the older lunar basins. A stratigraphically intermediate basin, such as Nectaris, may serve as a diagnostic test for the cataclysm. An older age of >4.1 Ga would weaken the scenario of a cataclysm. In addition, the South-Pole Aitken basin is stratigraphically the oldest preserved basin on the Moon, and its age would provide strong evidence for a terminal cataclysm if it is very young (i.e., ~4 Ga; [17]). Quantitative ages for these basins would vastly improve our understanding of the lunar early impact history.

**References:** [1] Morbidelli A. et al. (2018) Icarus, 305, 262-276. [2] Bottke W. F. and Norman M.D. (2017) Annual Review of Earth and Planetary Sciences, 45, 619-647. [3] Hartmann W. K. (2019) Geosciences, 9(7), 285. [4] Neukum G. (1983) Univ. of Munich, 1–186. [5] Ivanov B. A. (2001) Space Science Reviews, 96(1), 87–104. [6] Michael G. and Neukum G. (2010) Earth and Planetary Science Letters, 294(3–4), 223–229. [7] Morbidelli A. et al. (2012) Earth and Planetary Science Letters, 355–356, 144–151. [8] Tera F. et al. (1974) Earth and Planetary Science Letters, 22(1), 1–21. [9] Cohen B. A. (2000) Science, 290(5497), 1754–1756. [10] Fernandes V. A. et al. (2013) Meteoritics and Planetary Science, 48(2), 241–269. [11] Michael G. et al. (2018) Icarus, 302, 80–103. [12] Liu T. et al. (2020) Icarus, 114206. [13] Orgel C. et al. (2018). Journal of Geophysical Research: Planets, 123(3), 748–762. [14] Cherniak D. and Watson E. (2001) Chemical Geology, 172(1–2), 5–24. [15] Crow C. A. et al. (2017) Geochimica et Cosmochimica Acta, 202, 264–284. [16] Vanderliek D. M. et al. (2021) Earth and Planetary Science Letters, 576, 117216. [17] Norman M. D. (2009) Elements, 5(1), 23–28.